FP13 Measurement of Muon Properties Advanced Lab Course Physics

Names: Philipp Wendland and Jan Maintok
Date: February 2018

1 Abstract

Using a multilayer scintillator detector the lifetime τ_0 and magnetic moment μ_μ^{Bohr} of muons, the Fermi constant G_F and the parity violation in the weak interaction are analysed. By looking at the rates of events in each of the layers relative to each other information was gained about the energy of the incoming muons. The experiment gave

$$\begin{aligned}\tau_0 &= (2.28 \pm 0.05_{\text{stat}} \pm 0.22_{\text{sys}})\mu\text{s},\\ G_F &= (1.14 \pm 0.03_{\text{stat}} \pm 0.11_{\text{sys}}) \cdot 10^{-5}\text{GeV}^{-2},\\ \mu_\mu^{\text{Bohr}} &= (3.82 \pm 0.26_{\text{stat}} \pm 0.39_{\text{sys}}) \cdot 10^{-26}\frac{J}{T}.\end{aligned}$$

Also, the parity violating processes could be observed.

2 Introduction

The muon was first discovered in 1936 when researchers at Caltech observed a particle that came from cosmic radiation and that, when passing a magnetic field, curved less than an electron but more than a proton and was assumed to have the same charge as the electron. This particle was first thought to be the so-called Yukawa particle, which today is known as a pion, because of the similar mass. Nowadays muons play a significant role in particle physics, as it is - as far as we know - an elementary particle with a mass small compared to typical energies in modern particle physics experiments. For example muons played a role in the discovery of the higgs boson (8,9), as one of the clearest decay channels for the higgs boson is into two Z bosons which in turn decay into four leptons. Muons were also used in the Rossi-Hall experiment (1941) to confirm time dilation as predicted by Einstein's theory of special relativity. What also makes them interesting, is the fact that the production as well as the decay of cosmic muons violates the parity symmetry that was long thought to be a universal symmetry of the universe. This parity violation in the weak interaction as well as other basic properties of the muon will also be analysed in this experiment. 2

3 Theory

3.1 The muon

The muon is an elementary particle. In the Standard Model of particle physics it belongs to the group of leptons. It has an electric charge of -1e and spin $s = \frac{1}{2}$, but is approximately 207 times heavier than the electron ($m_\mu = 105.7\text{MeV} / c^2$) [2].
Cosmic muons are produced from decaying pions and kaons, which in turn are produced by energetic protons coming from primary cosmic rays. The production of muons from decaying pions can amongst others occur as follows

$$\pi^+ \rightarrow \mu^+ + \nu_\mu \tag{3.1}$$

$$\pi^- \rightarrow \mu^- + \bar{\nu_\mu}. \tag{3.2}$$

The primary cosmic radiation is positively charged. Hence the decay into positive muons is favourable.
Muons have an average lifetime of $\tau = 2.19\mu$s [1]. A muon decays into an electron and two neutrinos via the weak interaction

$$\mu^- \rightarrow e^- + \nu_\mu = +\bar{\nu_e} \tag{3.3}$$

$$\mu^+ \rightarrow e^+ + \nu_e = +\bar{\nu_\mu}. \tag{3.4}$$

With the average lifetime τ the decay follows an exponential law

$$N(t) = N(t_0)e^{-\frac{t-t_0}{\tau}}. \tag{3.5}$$

Both positive and negative muons can decay as free particles or by capturing an electron and thus forming the so called muon atom. Negative muons can however also be captured by atomic nuclei. This effectively reduces the lifetime of negative muons to

$$\frac{1}{\tau} = \frac{1}{\tau_0} + \frac{1}{\tau_c}, \tag{3.6}$$

with τ_0 and τ_c being the muon lifetime and the lifetime of a captured muon respectively. With a measurement of the lifetime τ_0 and knowledge of the muon mass m_μ the Fermi constant G_F can be determined

$$G_F^2 = \frac{192 \cdot \pi^3 \cdot \hbar}{\tau_0 \cdot (m_\mu c^2)^5}. \tag{3.7}$$

3.2 Parity violation

A parity transformation refers to the flip in the sign of spacial coordinates [3]. Applying a parity transformation to a particle with momentum **p** and spin **s** results in a change of sign in **p** and an unchanged spin.
The relative direction between momentum and spin is captured by the concept of helicity. If both momentum and spin point in the same direction, one speaks of a helicity of +1 (right-handed). If they point in different directions the helicity is -1 and one speaks

of a left-handed particle.
Now, the weak interaction couples only to the left-handed particles and the right-handed part of anti-particles. Assuming that the particle is massless, such that helicity and charlity coincide. As described above, cosmic muons are produced by decaying pions. Pions have spin 0, thus the spin has to be conserved in its decay. This leads to two different configurations. One, where the helicity of the products (the muon and the muon-neutrino, cf. Eq. 3.2, 3.1) is +1 and one, where it is -1. Since the neutrino is almost massless, the weak interaction suppresses the production of left-handed neutrinos. This gives the muons a preferred spin direction, thus violating parity. By measuring the polarisation of incoming muons the asymmetry in the distribution of left- and right-handed muons can be determined. Thus giving proof of the parity violation of the weak interaction.

3.3 Magnetic moment

The magnetic moment of a muon is given by

$$\mu_\mu = g_\mu \cdot \mu_\mu^{Bohr} \cdot \mathbf{s} \tag{3.8}$$

where the Bohr-magneton is given as $\mu_\mu^{Bohr} = \frac{e\hbar}{2m_\mu}$. If the spin of the muon is perpendicular to an external magnetic flux $\mathbf{B}$, the magnetic moment of the muon performs a Larmor precession with

$$w_{Larmor} = \frac{g \cdot \mu_\mu^{Bohr} \cdot \mathbf{B}}{\hbar}. \tag{3.9}$$

This precession is observable by measuring the time dependence of the asymmetry in the decay of the cosmic muons. This is made possible by the fact that in a μ^+-decay the positron is mostly emitted in the direction of the muon spin [1].

4 Experimental Setup

4.1 Hardware

The detector is made up of layers of scintillators. These are read out by a photomultiplier and energy absorbing metal plates. Between the first and the second scintillator layer there is a 2.5 cm thick iron plate, between the others there are 8 cm thick aluminium plates.

4.1.1 Scintillation detector

A scintillation detector consists of a scintillator and a photomultiplier. When the scintillator is hit by a (charged) particle it absorbs its energy and emits it in the form of electromagnetic radiation, mostly visible or UV light. To be able to detect how much energy is being absorbed the light reaches a photomultiplier. Due of the photoelectric effect materials emit electrons when light with a certain frequency hits the material.

These electrons are then focused and an electric pulse can be measured and analysed. This in turn gives information about the original particle that struck the scintillator.

4.2 Expected energy loss in the detector

Using the simple model, that the muons are roughly minimum ionizing particles (MIPS), which is reasonable in the range of expected muon energies (average of 2 GeV 1), and therefore loose around 2 MeV$\frac{\text{cm}^2}{\text{g}}$, we can calculate the average energy loss for the muons in the detector (Fig. 4). In the iron plate they loose $\approx$ 39 MeV and in the three aluminium plates they loose $\approx$ 130 MeV. Assuming that there is roughly 1 m of concrete above the experiment they will approximately loose an additional 400 MeV there. In total the muons will on average loose less than 600 MeV of energy. Knowing that the average energy of the muons is 2 GeV, one would expect most muons to just pass the whole detector.

4.3 Relative muon rates due to the detector geometry

To find out whether this hypothesis is valid, it is important to know what relative rates one would expect due to the geometry of the detector and the trigger setup only. For this a Monte Carlo simulation was made. It is assumed here, that the arrival directions of the muons are isotropically from above. This is a reasonable assumption, because to be detected the muons have to come from low zenith angles anyway and nonisotrosopy only plays a significant role for high zenith angles, since there muons have to travel a longer distance through the atmosphere, which reduces their number.
If you had a flat detector (so only one of the three detector planes), the muonflux mf for a certain zenith angle can be calculated as

$$mf(\theta) = \int \cos^2\theta \mathrm{d}\theta = \frac{\theta}{2} + \frac{1}{4}\sin(2\theta) \tag{4.1}$$

The probability for a muon to be detected also depends on the intersection area of the top and the bottom plane as seen from the muon. This is illustrated by Fig. 1.

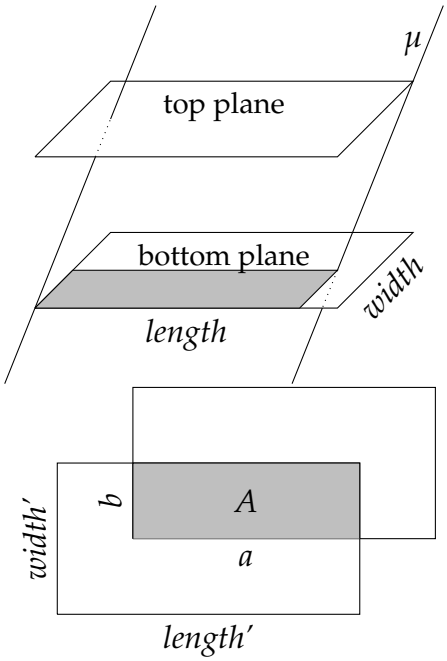

Fig. 1: *Top:* side view of projected plane intersection. *Bottom:* plane intersection as seen from a certain direction.

This area can be calculated as

$$a = length - heigth\,|\sin\phi|\,\tan\theta, \tag{4.2}$$

$$b = width - heigth\,|\cos\phi|\,\tan\theta, \tag{4.3}$$

$$A(\theta,\phi) = \begin{cases} ab; & \text{for } a > 0 \text{ and } b > 0, \\ 0; & \text{otherwise,} \end{cases} \tag{4.4}$$

Last but not least one has to take into account the detection efficiencies e of the detector planes. Since an event is only saved if a signal is detected in the first two scintillators, the efficiency for these has to be set to 1. For the other planes the measured value is taken. The expected rate of the measurement in the nth scintillator is therefore proportional to

$$r \propto mf(\theta) \cdot A(\theta,\phi) \cdot e \tag{4.5}$$

For the simulation isotropic values for the zenith and polar angle are generated and the measurement rate (in arbitrary units) is calculated for the different heights (distance from the top scintillator to the scintillator of interest) and therefore scintillators. All of these rates are added together for each of the scintillators. By dividing the rates of the top two scintillators by the rates of the other scintillators the relative rates that should be observed due to the detector geometry can be calculated. The result can be seen in Fig. 2

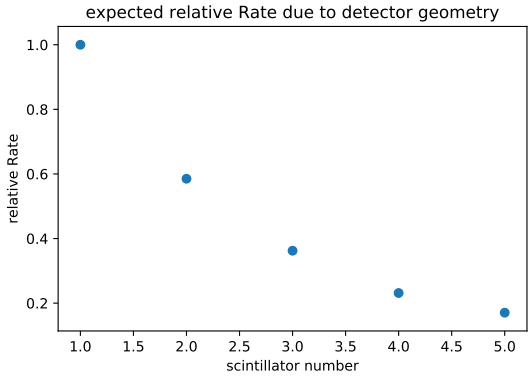

Fig. 2: Relative Rates

5 Results

The oscilloscope is connected to the output of the PMs of the scintillators and signals of roughly 50 to 500mV can be observed, whereas really big pulses do not occur very frequently. In Fig. 3 one can see a typical pulse of the scintillator. Changing the terminating resistor from 50Ω to 1MΩ does not have a huge impact on the observed pulses, it does give a little overshoot after the pulse gets back to zero though (See Fig. 3).

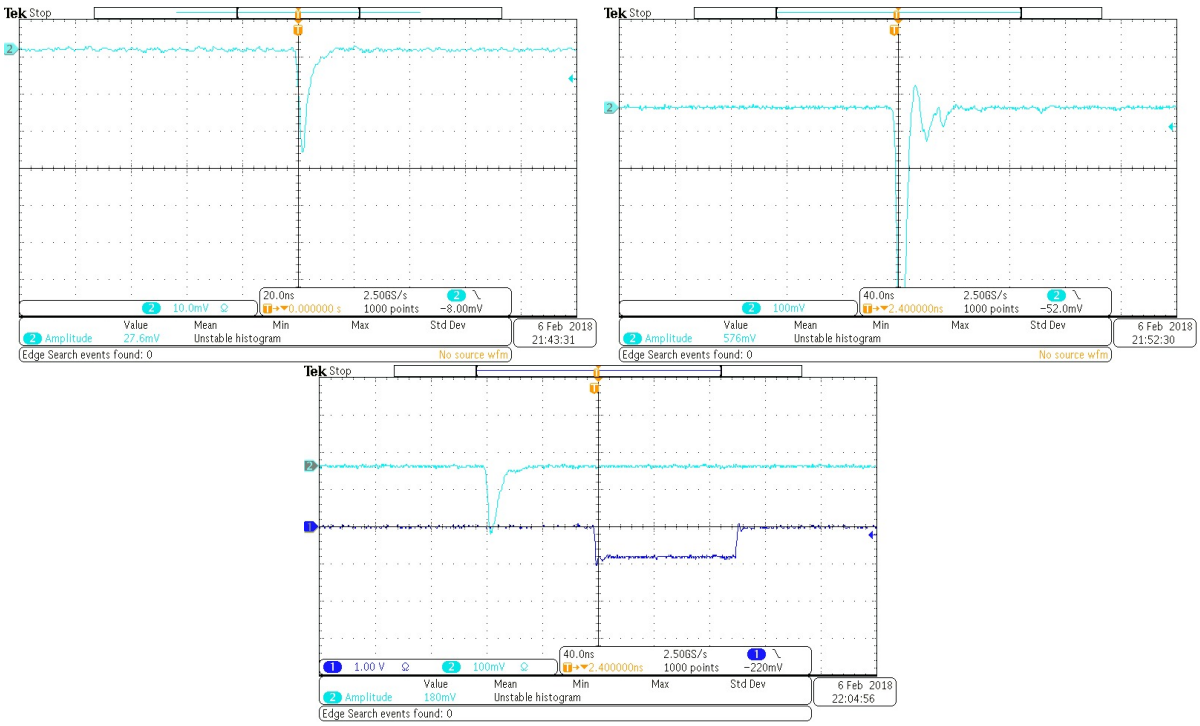

Fig. 3: *Left:* typical pulse from the scintillator, *Right:* Pulse with 1MΩ terminating resistor, *Pulse and discriminator output*

1. How are photons detected in a photomultiplier?

2. How are the photons generated in the scintillator?
   The answers to the last two questions can be found in section 3 from above.

3. How much energy do relativistic particles such as muons from cosmic radiation deposit in a scintillator?
   That depends on the type of scintillator. The mean energy that is lost by a high energy muon is described by the Bethe-Bloch equation (5.1).

$$-\left\langle \frac{dE}{dx} \right\rangle = \frac{4\pi}{m_e c^2} \cdot \frac{nz^2}{\beta^2} \cdot \left(\frac{e^2}{4\pi\varepsilon_0} \right)^2 \cdot \left[\ln\left(\frac{2m_e c^2 \beta^2}{I \cdot (1-\beta^2)} \right) - \beta^2 \right] \tag{5.1}$$

   where z is the charge, E the energy, x the distance the muon travels into a target of electron number density n and mean excitation potential I, c is the speed of light and ϵ_0 the vacuum permittivity, $\beta = \frac{v}{c}$, e and m_e the electron charge and rest mass respectively. The energy dependence of the energy loss as described by Bethe-Bloch can be seen in Fig. 4 (Here the energy loss is shown for μ^+ in copper, for different materials this curve slightly changes).

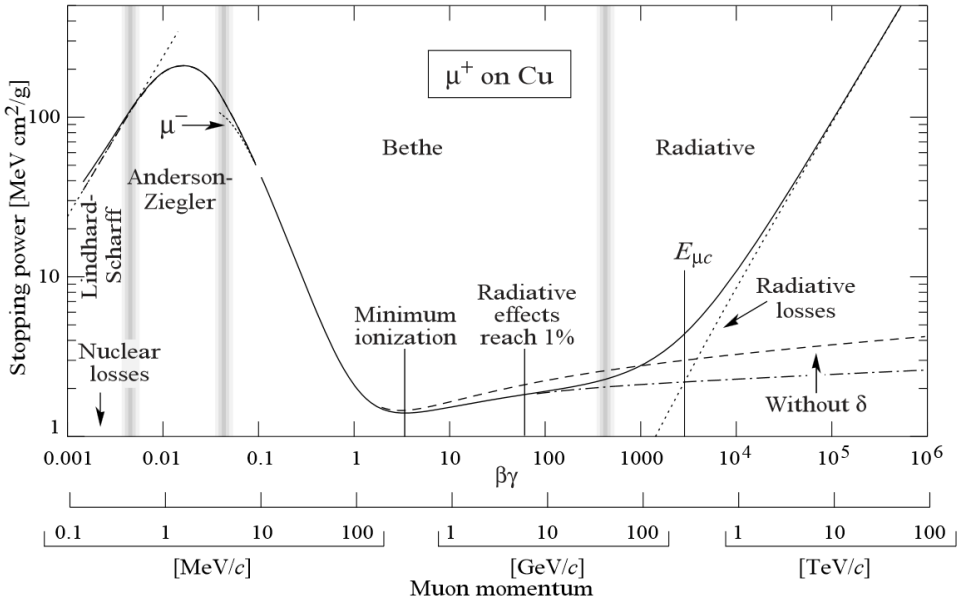

Fig. 4: Bethe-Bloch curve, taken from 6

For muons of energy 1 GeV we get $\beta\gamma \approx 10$ which means that $\left\langle \frac{\mathrm{d}E}{\mathrm{d}x} \right\rangle \approx 2\frac{\mathrm{MeV \cdot cm^2}}{g}$. Unfortunately the exact scintillator type is not given. According to the Particle Data Group (4) densities for organic scintillators are around $1\frac{\mathrm{g}}{\mathrm{cm}^3}$ while densities for inorganic scintillators are in the range from $4 - 8\frac{\mathrm{g}}{\mathrm{cm}^3}$. This means an energy loss of approximately $\left\langle \frac{\mathrm{d}E}{\mathrm{d}x} \right\rangle \approx 1 - 16\frac{\mathrm{MeV}}{cm}$. Since the scintillators are each 1cm thick, this is also the mean energyloss per scintillator plane. This loss is obviously distributed around this mean value according to the Landau distribution. Also one has to note, that most muons that are used for the measurement are those, that decay inside the detector. As discussed above these are very low energy muons, high energy muons (1GeV) will not be stopped by the detector. For minimum ionizing particles (MIPS), muons with $\beta\gamma \approx 3 - 4$ so energies of around 300-400MeV will probably

deposit only about half this energy, whereas muons of even lower energies will deposit much more energy due to the rapid increase in energy loss below $\beta\gamma = 3$.

4. Which impact has the terminator on the waveform?
   It does not have a huge impact though having the smaller resistor reduces the overshoot and oscillating behaviour that can be seen with the large resistor.
5. How do pulses from photomultiplier tubes look like?
   A typical pulse from the photomultiplier (PMT) can be seen in Fig. 3
6. What determines the height of these pulses?
   The height of these pulses depends on various parameters. Most importantly it depends on the number of photons, which is proportional to the energy loss in the scintillator (as discussed above) that hit the photocathode of the PMT. More primary photoelectrons will create a stronger signal. (The integrated signal should roughly be proportional to the number of primary photoelectrons). It also depends on the multiplicity of the PMT, which in turn depends on the voltage applied to the electrodes in the PMT as well as the number, type and geometry of the dynodes.

Next the thresholds are changed and a lower threshold (absolute value, since the pulses are negative) yields a higher rate but also seems to give an output signal if there is no clear signal. A higher threshold on the other hand yields a lower rate of very high peaked signals. Thresholds of around -10mV seemed to be a good compromise. The pulse heights still varied between 50 to 500mV. The signal of the discriminator was slightly shifted from the scintillatorsignal by around 80ns and had a width of around 102ns.

1. What is the functionality of the discriminators?
   The discriminators make sure, that the timing of the different signals is done consistently 5. If the time when the threshold is passed by a signal would be taken, higher signals would give a signal slightly earlier than lower signals, since the rise to the threshold is faster if the signal is higher. A constant fraction discriminator solves this problem in that it gives a signal in the moment when the signal is a certain fraction of its way up to the peak (under the condition, that the threshold is passed at all). Thus giving better timing of the signals, which is crucial for lifetime measurements.
2. Which impact has changing the thresholds?
   The impact of the thresholds is already discussed above.

The scintillators have a width of 32.5 ± 0.5cm and a length of 82 ± 2cm. The length was not easily measurable since it was not clear where the scintillator ended and the readout started. The top of the photomultipliers where measured to be at $9.5 \pm 0.5; 85.0 \pm 0.5; 76.0 \pm 0.5; 66.0 \pm 0.5; 56.5 \pm 0.5; 47.5 \pm 0.5; 37.5 \pm 0.5; 28.0 \pm 0.5$ above ground.

The counting rates were found to be around 100Hz for the thresholds used as above. For measurements that had the layer above and below as a reference, the detection efficiency was measured (assuming, that a signal in the two reference plains at the same time that does not give a signal in the measured layer means that a signal should have been observed but hasn't) to be 96.6% for scintillator 1, 96.2% for scintillator 2, 96.1% for scintillator 3 and 91.6% for scintillator 4. The thresholds where kept at -10mV since changing them did not improve the efficiency for scintillator 4.

After this the rates drastically changed, so that we recalibrated the thresholds to -10mV for scintillator 0, -10mV for scintillator 1, -15mV for scintillator 2, -17mV for scintillator 3, -15mV for scintillator 4 and -30 for scintillator 5. This gave us rates of 124.5Hz for scintillator 0, 128.4Hz for scintillator 1, 119.8Hz for scintillator 2, 140.3Hz for scintillator 3, 122.4Hz for scintillator 4 and 113.2Hz for scintillator 5. With these we got efficiencies of 97.5 (sc.1), 96.5 (sc.2), 94.9 (sc.3), 95.4 (sc.4) respectively.
At these rates we expect a rate of random coincidences of around

$$R_{12} = R_1 R_2 \Delta t \approx 0.00144\text{Hz} \tag{5.2}$$

which is only roughly 0.0012% of all events and can therefore be neglected.

5.1 Measurement of the muon lifetime

The LabView program Lebensdauer.vi is then started and run for two days to acquire data. It also gives some online histograms that show the number of hits in each of the layers, the number of slices per event (e.g. the number of time slots in which signals have been registered for the whole detector) as well as some overview over the daq-session (elapsed time, number of events etc.). It also gives a rough representation of the discriminator output signals of all detector planes in different time slots.
A muon decay will here be seen as a signal that crosses some detector planes (e.g. there is a signal in all of them at the same time) and an additional signal in the same (decay upwards) or the one below (decay downwards) the last layer that has been hit. A delayed signal above the last layer that has been hit is most likely an afterpulse. These afterpulses can unfortunately also create false signals with the same characteristics as a muon signal which means the afterpulse spectrum has to be subtracted from the muon spectrum later on. All other signals will not be used for further analysis.

The data was then analysed using a pre-written C++ program. The only thing that had to be added was an improved method to get the afterpulses, that have been described above. A basic method was already done that looked at the events that had a muon going through all the layers. This means that a signal in any but the last detector planes (this could be a decay upwards just below the last detector plane) is most likely an afterpulse. However one can improve on this by also looking at all the events and registering afterpulses for all the planes above the last one that has been hit. Since the thickness of the absorbing metals matches the average range of the electrons coming from the muon decay it is likely that these kind of signals are afterpulses and not from a muon. Also a function that finds decays downwards had to be implemented and can be seen below.

```
int fp13Analysis::findDecayDownward(int timeBin){
    if ((nLayers - 1) == lastMuonLayer)
        return -1;
    if ((1 << (lastMuonLayer+1)) \& detectorHitMask[timeBin])
        return lastMuonLayer;
  return -1;
}
```

The more general function for the after pulses can be seen below.

Layer	N_{stop}	N_{start}	Scaling factor s (up)	Error δ_s	s (down)
1	687990	1917633	0.3588	0.0005	undefined
2	476842	1440791	0.3310	0.0006	0.0168
3	336548	1104243	0.3048	0.0006	0.0171
4	248892	855351	0.2910	0.0007	0.0160
5	855351	0	undefined	undefined	undefined

Fig. 5: Scaling factor for the correction for the after-pulses histogram.

```
int fp13Analysis::findAfterpulsesImproved(int timeBin, int startLayer) {
    if (-1 == startLayer)
      startLayer = lastMuonLayer;
    for (int iLayer = startLayer -1 ; iLayer >= 0; iLayer--) {
        if ((1 << iLayer) & detectorHitMask[timeBin])
          return iLayer;
    }
  return -1;
}
```

The program is then executed as described in the manual, which automatically fills several histograms. As described above afterpulses can also wrongly be identified as muon decays which means that the afterpulse spectrum has to be subtracted from the muon spectrum. To get the correct lifetime. The number of actual muons which decay upwards is given by

$$N_\mu^0 = N_{tot} - s \cdot N_{NP} = N_{tot} - \frac{N_{i,stop}}{N_{NP,start}} \cdot N_{NP} \tag{5.3}$$

where N_{tot} is the total number of muon candidates, $N_{i,stop}$ the number of signal events which only give signal until layer i, $N_{NP,start}$ the number of events that have been analysed for afterpulses and N_{NP} the number of after pulses. The ratio $\frac{N_{NP}}{N_{NP,start}}$ therefore describes the probability that after the passage of a particle, an after pulse was produced. Since N_{tot} and N_{NP} depend on the decay time, the scaling factor $s = \frac{N_{i,stop}}{N_{NP,start}}$ is calculated to subtract the afterpulse spectrum from the muon candidates. The scaling factors can be seen in Tab. 5. For the decays downwards it is a little bit more complicated. For a decay down candidate to be an afterpulse, it is necessary that the muon should have produced a signal in the plane that is the same as the afterpulse but did not register. This is described by the efficiency that has been determined above. The scaling factor is then given by $s = \frac{N_{i-1,stop}}{N_{NP,start}} \cdot \frac{1-\epsilon}{\epsilon}$, where ϵ is the efficiency. The error of the scaling factor (will be important later on for the up decay) is given by $\delta_s = s\sqrt{\frac{1}{N_{stop}} + \frac{1}{N_{start}}}$ since N_{stop} and N_{start} can be assumed to be Poisson distributed.

This corrected spectrum for the second detector plane can be seen in Fig. 6

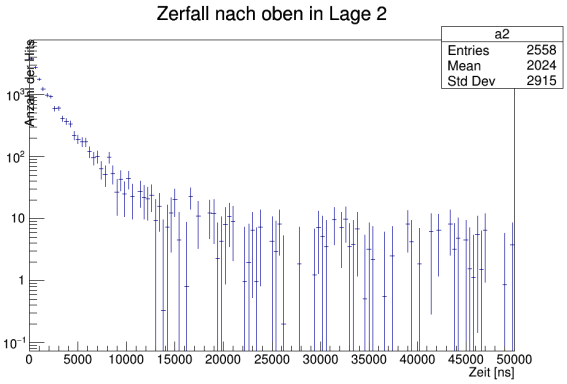

Fig. 6: corrected muon spectrum for the second detector layer

In Fig. 7 one can see the different spectra for the different detector planes.

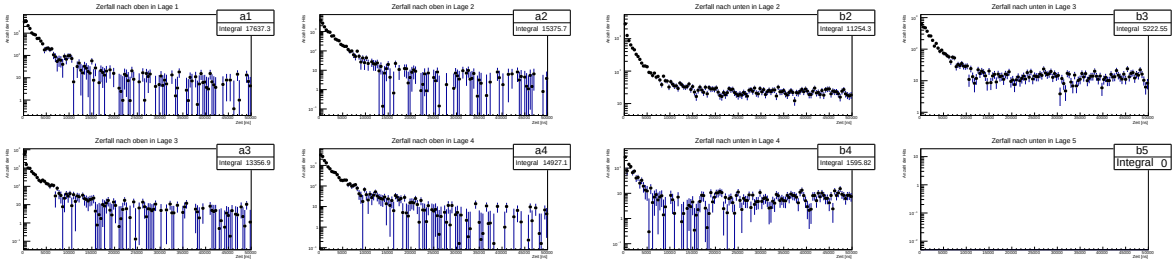

Fig. 7: muon decay spectra for the different detector planes, *Left:* decay up, *Right:* decay down

The given macro Weiteres.C was analysed, no unexpected behaviour was observed. Fig.8.

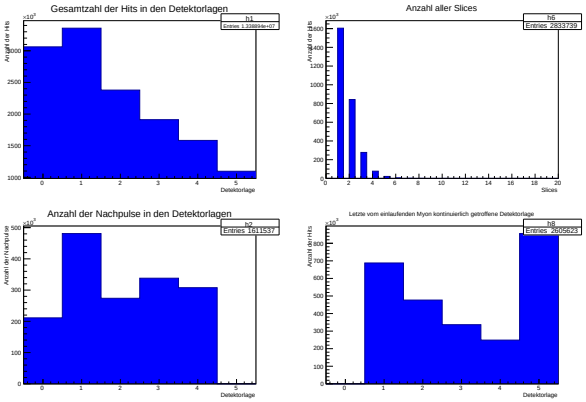

Fig. 8: *Top Left:* total number of hits in each of the detector layers, *Top Right:* number of time slices with a pulse, *Bottom Left:* number of after pulses in each of the detector layers, *Bottom Right:* last layer that was continuously hit by the muon.

To this data we now fit a function of the form

$$N(t) = N(\mu)e^{-\frac{t}{\tau_0}} + N_{BG}. \tag{5.4}$$

This fit gives significantly different lifetimes depending on the fitrange as can be seen in Tab. 9.

Measured quantity	1000 - 20000	300 - 40000	300 - 20000	1000 - 40000	2000 - 40000
τ_0 (up)	1.93 ± 0.04	1.87 ± 0.04	1.74 ± 0.04	2.09 ± 0.05	2.50 ± 0.08
χ^2_{red} (up)	2.2	3.5	4.0	2.3	1.6
τ_0 (down)	1.91 ± 0.05	1.91 ± 0.04	1.86 ± 0.04	1.97 ± 0.05	2.21 ± 0.08
χ^2_{red} (down)	1.9	1.4	2.0	1.4	1.1
τ_0 (combined)	1.93 ± 0.04	1.88 ± 0.03	1.76 ± 0.03	2.07 ± 0.04	2.44 ± 0.06
χ^2_{red} (combined)	2.6	3.9	4.6	2.6	1.7

Fig. 9: Fits for different Fitranges using Fit 5.4.

The plots for layer 2 to these fits can be seen in Fig. 10

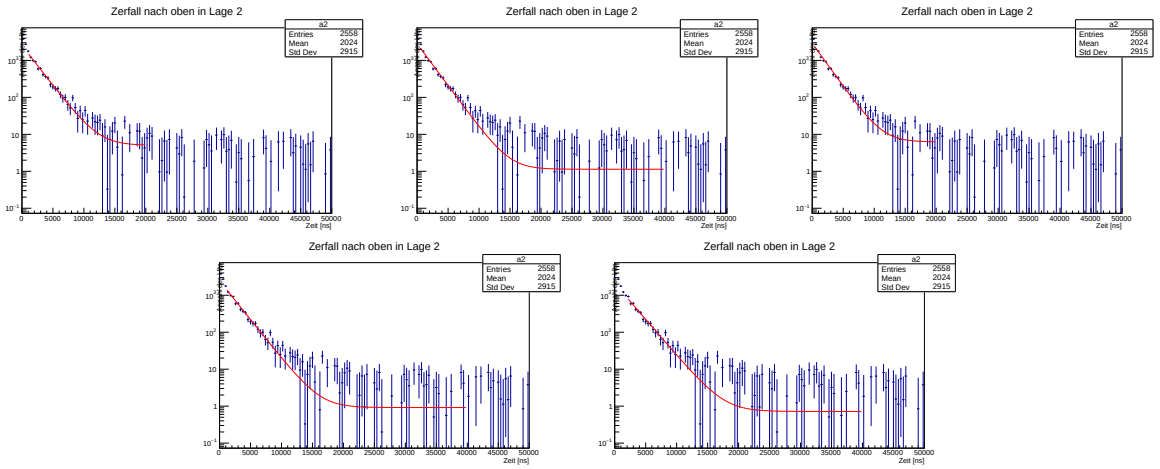

Fig. 10: Fit using different fitranges

To take into account that the negative muons can also be captured by atoms one has to modify the fit function slightly to

$$N(t) = N_{\mu^+} \cdot e^{-\frac{t}{\tau_0}} \left(\frac{1}{f} e^{-\frac{t}{\tau_C}} + 1 \right) + N_{BG} \tag{5.5}$$

where f is the ratio $\frac{N_{\mu^+}}{N_{\mu^-}}$.

Again the lifetime was quite dependent on the fitrange, the results can be seen in Tab. 11

In Fig. 12 one can see one typical graph from these fits.

Measured quantity	1000 - 20000	300 - 40000	300 - 20000	1000 - 40000	2000 - 40000
τ_0 (up)	2.20 ± 0.07	2.16 ± 0.05	2.00 ± 0.05	2.40 ± 0.06	2.7 ± 0.7
τ_c (up)	1.24 ± 0.26	1.00 ± 0.13	0.89 ± 0.13	1.43 ± 0.21	1.50 ± 0.11
χ^2_{red} (up)	1.5	2.3	2.2	1.7	1.4
τ_0 (down)	2.20 ± 0.07	1.91 ± 0.04	2.21 ± 0.05	2.26 ± 0.07	2.37 ± 0.08
τ_c (down)	1.34 ± 0.31	0.1 ± 1.0	1.38 ± 0.27	1.38 ± 0.29	1.5 ± 0.9
χ^2_{red} (down)	1.4	1.5	1.4	1.1	1.0
τ_0 (combined)	2.20 ± 0.06	2.17 ± 0.04	2.04 ± 0.04	2.37 ± 0.05	2.62 ± 0.07
τ_c (combined)	1.25 ± 0.23	1.03 ± 0.12	0.92 ± 0.12	1.42 ± 0.19	1.50 ± 0.10
χ^2_{red} (combined)	1.6	2.4	2.3	1.9	1.5

Fig. 11: Fits for different Fitranges using Fit 5.5.

Measured quantity	$f = 1.275$	$f = 1.225$	$f = 1.325$	$f = 1.175$	$f = 1.375$
τ_0 (combined)	2.20 ± 0.06	2.21 ± 0.06	2.19 ± 0.05	2.22 ± 0.06	2.18 ± 0.05
τ_c (combined)	1.25 ± 0.23	1.25 ± 0.22	1.25 ± 0.23	1.25 ± 0.22	1.26 ± 0.23
χ^2_{red} (combined)	1.6	1.6	1.6	1.6	1.7

Fig. 13: Variation of Parameter f.

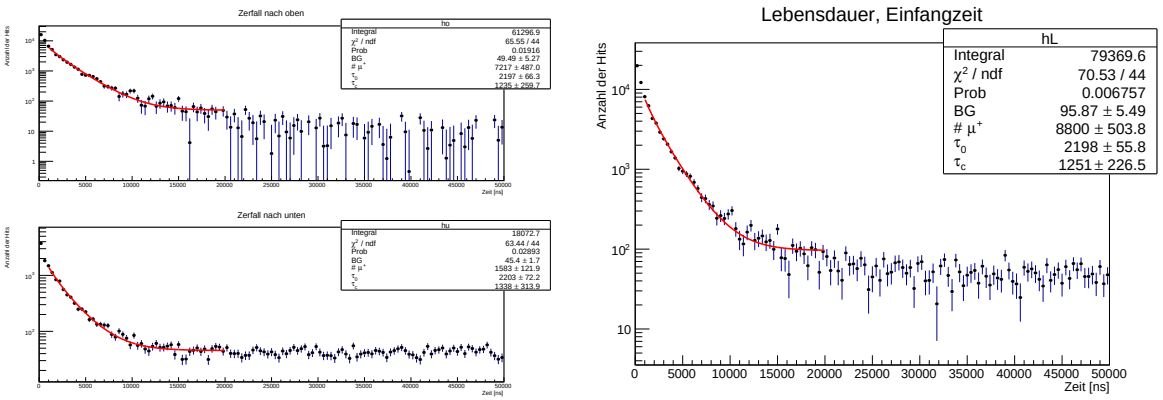

Fig. 12: Fit to the data using improved formula *Left:* up and down decays, *Right:* combined decays

The parameter f was then changed to find out its systematic impact, the results can be seen in Tab. 13

The scaling factors are then systematically changed by $\pm 1\sigma$, the results can be seen in Tab. 14

Measured quantity	$s' = s$	$s' = s - 1\sigma_s$	$s' = s + 1\sigma_s$
τ_0 (combined)	2.20 ± 0.06	2.20 ± 0.06	2.20 ± 0.06
τ_c (combined)	1.25 ± 0.23	1.25 ± 0.22	1.25 ± 0.23
χ^2_{red} (combined)	1.6	1.6	1.6

Fig. 14: Variation of Parameter the scaling factors.

5.2 Measurement of the muon polarisation

Next a measurement with a magnetic field of 40mT parallel to the scintillator planes was applied and data is acquired over the weekend. As described above the muons are polarised, e.g. their spin is preferably downwards. This spin will now precess with the Larmor frequency. Because the decay of the muon is favoured to be in the direction of the spin, the counting rate should periodically change

$$Z^{with}(t) = Z_0 \cdot e^{-\frac{t}{\tau}} \cdot (1 + P \cdot A \cdot \cos(\omega_{Larmor} \cdot t + \phi)) \tag{5.6}$$

if a magnetic field is present. Because the counting rate without a magnetic field is given by

$$Z^{without}(t) = Z_0 \cdot e^{-\frac{t}{\tau}} \cdot (1 + P \cdot A \cdot \cos(\phi)) \tag{5.7}$$

we can look at

$$\frac{Z^{with}(t) - Z^{without}(t)}{Z^{with}(t) + Z^{without}(t)} \approx \frac{P \cdot A}{2} \cdot \cos(\omega_{Larmor} t + \phi) + c \tag{5.8}$$

to eliminate the exponential decay and find the Larmor frequency as well as the factor $P \cdot A$.

For this the scaling factors first have to be recalculated for the new dataset, as can be seen in Tab. 15

Layer	N_{stop}	N_{start}	Scaling factor s (up)	Error δ_s	s (down)
1	1538400	4445981	0.3460	0.0003	undefined
2	1065690	3380291	0.3153	0.0004	0.0165
3	769962	2610329	0.2950	0.0004	0.022
4	573869	2036460	0.2818	0.0004	0.0182
5	2036460	0	undefined	undefined	undefined

Fig. 15: Scaling factor for the correction for the after-pulses polarisation measurement.

In Fig. 17 one can see the asymmetry function including a fit for the relevant parameters. Unfortunately the errorbars are so big, that the fit does not give a significant result for the Larmor frequency. In Fig. **??** one can see the result if the afterpulse spectra are not subtracted from the muon spectra. Because they are present in both the spectra with a magnetic field as well as without they should cancel out and not have an effect on the outcome. This yields a much clearer result.

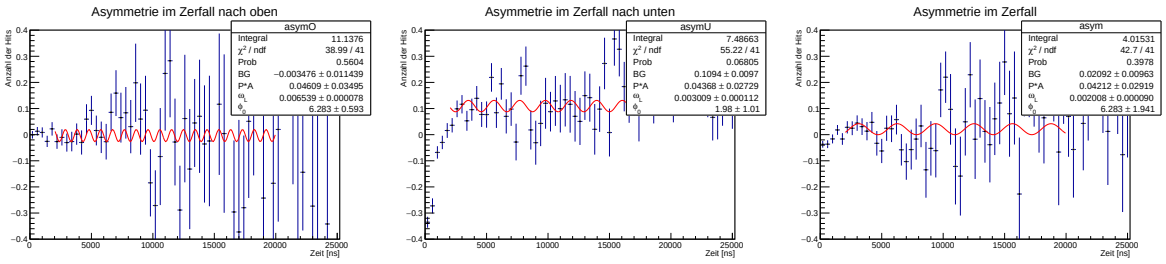

Fig. 16: Asymmetry in the muon decay, using corrected spectra *Left:* u decays, *Center:* down decays *Right:* combined decays

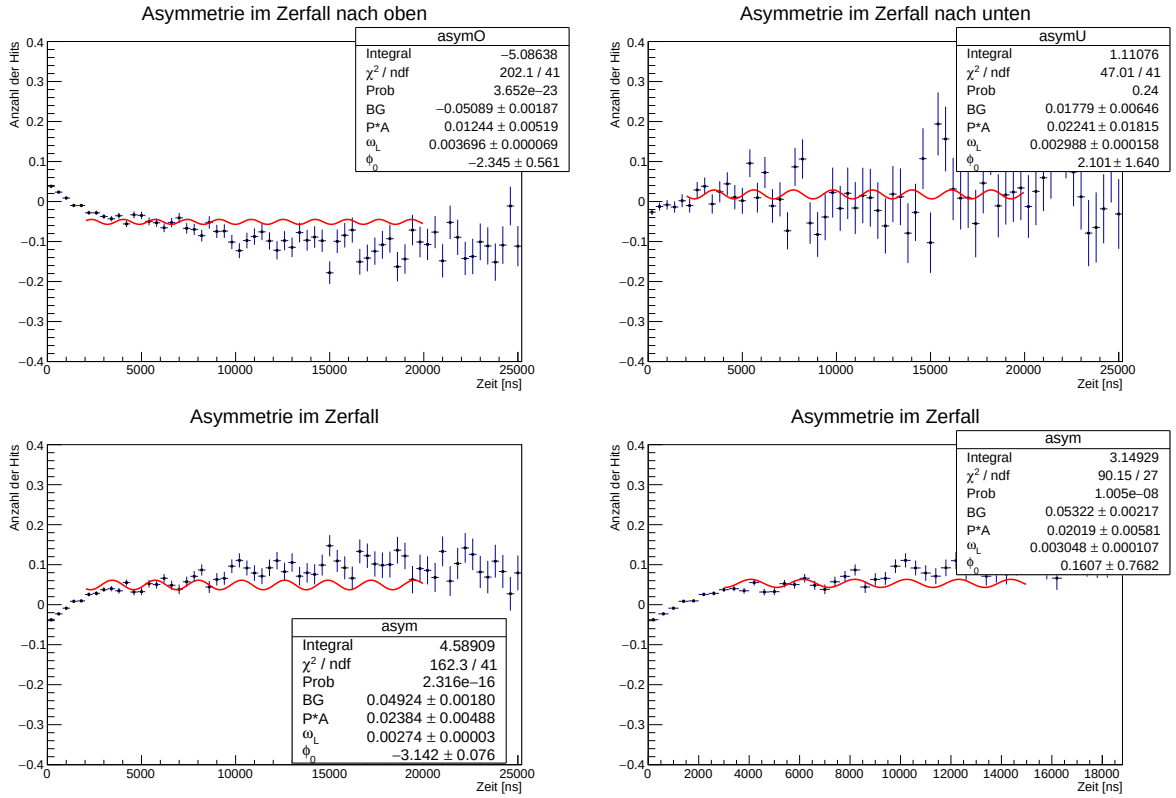

Fig. 17: Asymmetry in the muon decay using uncorrected spectra *Top Left:* up decays, *Top Right:* down decays, *Bottom Left:* combined decays, *Bottom Right:* combined decays, different fitrange

6 Analysis

From Tab. 9 one can see, that the measurement for the lifetime of muons significantly depends on the fitrange that is used for the analysis. One can also see, that the fits don't give an excellent χ^2_{red} which is an indicator for an imperfect model with some systematic effect not taken into account. The fits for the decays down are better than the decays up, this might be because the afterpulses play a much less significant role for the decays downwards. From the variation of the lifetime with the fitrange, one can estimate the systematic error by calculating the sample standard deviation ($\sigma_{sys} = \frac{1}{N-1}\sum_{i=1}^{N}(\tau_i - \bar{\tau})^2 = 0.26$). This yields

$$\tau_0 = (2.02 \pm 0.04_{\text{stat}} \pm 0.23_{\text{sys}})\mu\text{s}, \tag{6.1}$$

where the statistical error comes from the fit.

When taking into account the capturing of negative muons by atoms one gets slightly different results, as can be seen in Tab.11. Firstly one can see, that the χ^2_{red} is significantly reduced for all the fits, which shows, that the model has been improved by taking the capturing into account. Yet it is still a little bit too high, which hints at other systematic error sources that have not been taken into account. From this data we get analogously to before

$$\tau_0 = (2.28 \pm 0.05_{\text{stat}} \pm 0.22_{\text{sys}})\mu\text{s} \tag{6.2}$$

and

$$\tau_c = (1.22 \pm 0.15_{\text{stat}} \pm 0.25_{\text{sys}})\mu\text{s}. \tag{6.3}$$

The systematic error from the Parameter f and the scaling factors are negligible compared to the big systematic error from the fit range. Using

$$G_F^2 = \frac{192\pi^3\hbar}{\tau_0(m_\mu c^2)^5} \tag{6.4}$$

we get

$$G_F = (1.14 \pm 0.03_{\text{stat}} \pm 0.11_{\text{sys}}) \cdot 10^{-5} \frac{1}{\text{GeV}^2} \tag{6.5}$$

From the polarisation measurement we get a Larmor frequency of $\omega_L = 3.0 \pm 0.1_{\text{stat}}$MHz or $\omega_L = 2.74 \pm 0.31_{\text{stat}}$MHz depending on the fitrange. There has not been enough analysis done to systematically give a systematic error, it is estimated to be $\sigma_{sys} \approx$ 0.3MHz, yielding

$$\omega_L = 2.9 \pm 0.2_{\text{stat}} \pm 0.3_{\text{sys}}\text{MHz} \tag{6.6}$$

Where the systematic error sources that have been discussed above should play a role. Also not subtracting the after pulses could mess with the results. Using

$$\mu_\mu^{\text{Bohr}} = \frac{\hbar\omega_L}{gB} \tag{6.7}$$

we get

$$\mu_\mu^{\text{Bohr}} = (3.82 \pm 0.26_{\text{stat}} \pm 0.39_{\text{sys}}) \tag{6.8}$$

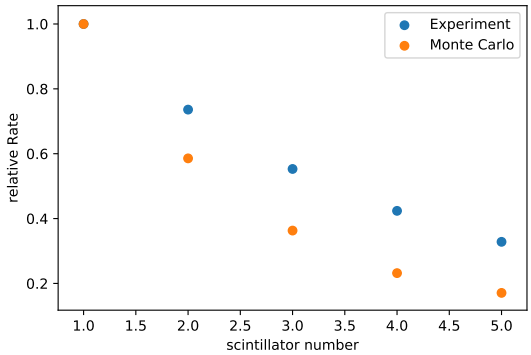

Fig. 18: Comparison of counting rates by layers

Also in Fig. 18 one can see how the relative rate changes with increasing detector layer. Relative to the number of events that pass the first scintillator we measure more events in the later detector layers relative to the number of events that would be expected from the detector geometry, as modelled by the Monte Carlo simulation. This indicates, that most muons are not stopped by the setup but will fly straight through the detector. Even if they are stopped, they are less likely to be stopped by the first few layers. This is the behaviour that would be expected, since most muons have more energy than what could be stopped by the detector, as has been predicted above.

7 Discussion and Summary

Our final result for the lifetime of muons ($\tau_0 = (2.28 \pm 0.05_{\text{stat}} \pm 0.22_{\text{sys}})\mu$s) deviates from the literature value ($\tau = 2.197\mu$s 1) by only 0.35σ. The Fermi constant obviously deviates from the literature value by the exactly the same margin (0.35σ). From the polarisation measurement we got $\mu_\mu^{\text{Bohr}} = (3.82 \pm 0.26_{\text{stat}} \pm 0.39_{\text{sys}}) \cdot 10^{-26} \frac{J}{T}$ which deviates from the expected value of $4.490 \cdot 10^{-26} \frac{\text{J}}{\text{T}}$ by 1.4σ. Given the low statistics on this part of the experiment this seems to be as good as one can expect the result to be. It is in the right order of magnitude though which does show that the muons reaching the earth are polarized and decay in a parity violating way.

In the experiment statistics play a big role so by doing longer measurements and taking more data one could probably improve the results. Lowering the statistical error might not seem to be as relevant compared to the big systematic errors, but by doing so one might be able to find an even better model, that takes into account even more of the systematics, than the one used in this analysis. The fact, that the fitrange had such a significant impact on the outcome of the experiment shows, that some systematic effect has not been taken into account yet. It would also be very interesting to analyse whether or not the after pulses depend on the energy or the energy loss of the muons. The events that have been used to get the afterpulse spectrum where from muons that flew further than the ones that could have created a false event, so the energy loss of the muon might be different in this case.

8 References and links

[1] Measurement of Muon Properties in the Advanced Students Laboratory; manual; Version 1.2.; Heidelberg University

[2] https://en.wikipedia.org/wiki/Muon

[3] https://en.wikipedia.org/wiki/Parity_(physics)

[4] http://pdg.lbl.gov/2015/reviews/rpp2015-rev-particle-detectors-accel.pdf

[5] https://en.wikipedia.org/wiki/Constant_fraction_discriminator

[6] http://pdg.lbl.gov/2009/reviews/rpp2009-rev-passage-particles-matter.pdf

[7] https://en.wikipedia.org/wiki/Higgs_boson

[8] https://arxiv.org/pdf/1207.7235.pdf

[9] https://arxiv.org/pdf/1207.7214.pdf